Journal of Biomolecular NMR, 5 (1995) 173–182
ESCOM

J-Bio NMR 241

Determination of $^{13}C^{\alpha}$ relaxation times in uniformly $^{13}C/^{15}N$-enriched proteins

Jan Engelke and Heinz Rüterjans*

Institut für Biophysikalische Chemie der Johann-Wolfgang Goethe Universität, Biozentrum N230, Marie-Curie Straße 9, D-60439 Frankfurt am Main, Germany

Received 18 May 1994
Accepted 7 October 1994

Keywords: 2D heteronuclear NMR; Protein dynamics; ^{13}C relaxation times

Summary

Relaxation times of $^{13}C^{\alpha}$ carbons of uniformly $^{13}C/^{15}N$-enriched probes have been investigated. The relaxation behaviour was analyzed in terms of a multispin system. Pulse sequences for the determination of T_1, T_2 and the heteronuclear NOE of $^{13}C^{\alpha}$ in uniformly $^{13}C/^{15}N$-enriched ribonuclease T1 are presented. The experiments performed in order to obtain T_1 and the heteronuclear NOE were similar to those of the corresponding ^{15}N experiments published previously. The determination of T_2 for the C^{α}-carbon in a completely labeled protein is more complicated, since the magnetization transfer during the T_2 evolution period owing to the scalar coupling of C^{α}-C^{β} must be suppressed. Various different pulse sequences for the T_2 evolution period were simulated in order to optimize the bandwidth for which reliable T_2 relaxation times can be obtained. A proof for the quality of these pulse sequences is given by fitting the intensity decay of individual ^1H-$^{13}C^{\alpha}$ cross peaks, in a series of (^1H,^{13}C)-ct-HSQC spectra with a modified CPMG sequence as well as a $T_{1\rho}$ sequence for the transverse relaxation time, to a single exponential using a simplex algorithm.

Introduction

In principle, NMR relaxation experiments can provide a detailed description of protein dynamics. In general, dynamic parameters are obtained from a determination of T_1, T_2 and NOE values (Richarz et al., 1980; Henry et al., 1986; Dellwo and Wand, 1989; Kay et al., 1989; Clore et al., 1990a; Palmer et al., 1991). Recently ^1H-detected sensitive one- and two-dimensional heteronuclear NMR experiments have been described for studying the relaxation properties of insensitive nuclei such as ^{15}N and ^{13}C (Kay et al., 1987,1989; Sklenář et al., 1987; Nirmala and Wagner, 1988,1989). While the ^{15}N relaxation experiments only provide information about backbone dynamics (Kay et al., 1989; Clore et al., 1990a,b; Barbato et al., 1992; Fushman et al., 1994), ^{13}C relaxation times can be used to study the motion of both the backbone and the side chains (Nicholson et al., 1992). In order to measure ^{13}C relaxation times, the use of unlabeled samples is certainly possible (Nirmala et al., 1988; Palmer et al., 1991,1993) but such an investigation is time-consuming and restricted to highly soluble proteins. The use of selectively ^{13}C-labeled proteins takes less time, but it requires the laborious synthesis or microbial production of selectively labeled samples (Nicholson et al., 1992). A uniformly ^{13}C-labeled protein which can also be used for assignment purposes is much easier to attain. Certainly, the use of such a sample for measuring ^{13}C relaxation times leads to two major problems: first, the presence of scalar couplings may induce relaxation of the second kind. Indeed, for measuring the transverse relaxation time a pulse sequence has to be developed which effectively suppresses the scalar C^{α}-C^{β} coupling during the T_2 evolution period. As a second aspect the kind of relaxation mechanism has to be considered: the nuclear spin relaxation of the amide nitrogen in a ^{15}N-labeled protein mainly stems from the dipole–dipole interaction between the amide nitrogen and its directly bound hydrogen. A minor part of the relaxation is caused by the ^{15}N chemical shift anisotropy (CSA). In this case the amide ^{15}N-^1H pair is an isolated

*To whom correspondence should be addressed.

AX spin system. In a completely $^{13}C/^{15}N$-labeled protein, the $^{13}C^{\alpha}$ nucleus is surrounded by several other nuclei with a nuclear spin and therefore CSA and various dipole–dipole interactions contribute to its relaxation. This environment implies that the relaxation of C^{α} cannot be described in terms of an AX spin system.

It should be mentioned that the relaxation of the glycine C^{α} carbon is different from that of all other $^{13}C^{\alpha}$ nuclei, because it relaxes according to an AX_2 spin system. Therefore, the pulse sequences described in this paper should not be applied to the $^{13}C^{\alpha}$ of glycine residues, since the different relaxation behaviour of the inner and outer lines of the AX_2 multiplet are not considered.

The present study follows two guidelines. First, the relaxation behaviour of $^{13}C^{\alpha}$ carbons of uniformly $^{13}C/^{15}N$-labeled proteins is analyzed from a theoretical point of view in order to decide whether relaxation times can be interpreted in terms of an isolated $^{13}C^{\alpha}$-$^{1}H^{\alpha}$ pair (AX spin system) or whether they have to be interpreted in terms of a multispin system. The second aim of the study is the development of pulse sequences for the determination of heteronuclear NOEs, T_1 and especially T_2 for C^{α} carbons of all amino acids, except glycine residues, in a uniformly $^{13}C/^{15}N$-enriched protein.

Analysis of the multispin relaxation of $^{13}C^{\alpha}$

In a uniformly $^{13}C/^{15}N$-labeled protein, various different spins are located in the vicinity of the $^{13}C^{\alpha}$ spin such that the analysis of its relaxation behaviour in terms of a multispin system should be considered. Since the CSA constant $\Delta\delta$ for C^{α} amounts to only about 30 ppm (Ye et al., 1993), the CSA relaxation mechanism can be neglected in most cases (Palmer et al., 1993). The relaxation owing to the dipole–dipole interaction of two nuclear spins A and B can be described in terms of the relaxation matrix elements (Bull, 1992). For $\omega_A = \omega_B$ or $\omega_A \neq \omega_B$ the direct dipole relaxation rate ρ_{AB} for the relaxation of spin A by spin B can be expressed as:

$$\rho_{AB} = c_{AB}^2 \cdot [0.5(1 + \cos^2\theta_A)\,[6J(\omega_A + \omega_B) + 3J(\omega_A) + J(\omega_A - \omega_B)] + \sin^2\theta_A[3J(\omega_B) + 2J(0)]] \quad (1)$$

For $\omega_A = \omega_B$ the cross-relaxation rate σ_{AB}, which controls the rate of the magnetization transfer between A and B (Neuhaus and Williamson, 1989), is:

$$\sigma_{AB} = c_{AB}^2 \cdot [6\cos\theta_A \cos\theta_B\, J(2\omega) + 3\sin\theta_A \sin\theta_B\, J(\omega) + (2\sin\theta_A \sin\theta_B - \cos\theta_A \cos\theta_B)\, J(0)] \quad (2)$$

For $\omega_A \neq \omega_B$ one obtains:

$$\sigma_{AB} = c_{AB}^2 \cdot [\cos\theta_A \cos\theta_B\,(6J(\omega_A + \omega_B) - J(\omega_A - \omega_B)] \quad (3)$$

where

$$c_{AB}^2 = \frac{\gamma_A^2 \gamma_B^2}{4\langle r_{AB}^3 \rangle^2}\left(\frac{h}{2\pi}\right)^2\left(\frac{\mu_0}{4\pi}\right)^2 \quad (4)$$

ω_A and ω_B are the resonance frequencies of two spins of the same ($\omega_A = \omega_B$) or different ($\omega_A \neq \omega_B$) nuclei species. θ_A (θ_B) denotes the angle between the magnetization vector of nucleus A (B) and the z-axis in the rotating frame. The values of c_{AB}^2 for the relevant contributions to the $^{13}C^{\alpha}$ relaxation are listed in Table 1.

In the case of transverse relaxation, the dipole–dipole relaxation rate ρ_{AB} for all relevant interactions is proportional to J(0) and therefore the contribution of each interaction depends only on the constant c_{AB}^2. Hence the transverse relaxation of the C^{α} is dominated by its covalently bound hydrogen and can be considered as an isolated AX spin system.

For the longitudinal relaxation phenomena (T_1 and the heteronuclear NOE), three dipole–dipole interactions have to be considered: the heteronuclear $^{13}C^{\alpha}$-$^{1}H^{\alpha}$ interaction, which is proportional to $J(\omega_C)$, and the two homonuclear $^{13}C^{\alpha}$-$^{13}C^{\beta}$ and $^{13}C^{\alpha}$-$^{13}C'$ interactions, which are proportional to J(0). In proteins J(0) is much larger than $J(\omega_C)$ and consequently the products $c_{C^{\alpha}C^{\beta}}^2 J(0)$ and $c_{C^{\alpha}C'}^2 J(0)$ become comparable to the product $c_{C^{\alpha}H^{\alpha}}^2 J(\omega_C)$.

In the following, the longitudinal relaxation of $^{13}C^{\alpha}$ in a uniformly $^{13}C/^{15}N$-enriched protein will be compared to that of an unlabeled protein. For the uniformly enriched protein, the longitudinal relaxation of $^{13}C^{\alpha}$ can be described with

$$\begin{pmatrix} \frac{d}{dt}C_z^{\alpha} \\ \frac{d}{dt}C_z^{\beta} \end{pmatrix} = \begin{pmatrix} -R_{C^{\alpha}} & -\sigma_{C^{\alpha}C^{\beta}} \\ -\sigma_{C^{\alpha}C^{\beta}} & -R_{C^{\beta}} \end{pmatrix} \cdot \begin{pmatrix} \langle C_z^{\alpha} \rangle - C_{eq}^{\alpha} \\ \langle C_z^{\beta} \rangle - C_{eq}^{\beta} \end{pmatrix} \quad (5)$$

where $R_{C^{\alpha}} = \rho_{C^{\alpha}H^{\alpha}} + \rho_{C^{\alpha}C^{\beta}} + \rho_{C^{\alpha}C'}$ and $R_{C^{\beta}} = \rho_{C^{\alpha}C^{\beta}} + \rho_{C^{\beta}C'} + \Sigma\rho_{C^{\beta}H^{\beta}}$. Note that cross relaxation between C^{α} and H^{α} is eliminated by proton saturation occurring during the relaxation period T. The cross relaxation with the carbonyl spin does not have to be considered either, because the aliphatic ^{13}C pulses were adjusted in such a way that the equilibrium magnetization of C' remains undisturbed ($\langle C_z' \rangle - C_{eq}' = 0$). Assuming that at the beginning of the longitudinal relaxation period $\langle C_z^{\alpha} \rangle$ (T = 0) = $C_z^{\alpha}(0)$ and $\langle C_z^{\beta} \rangle$ (T = 0) = $C_z^{\beta}(0)$, the solution for $\langle C_z^{\alpha} \rangle(T)$ is given by:

$$C_z^{\alpha}(T) = \left[C_{eq}^{\alpha} + (C_z^{\alpha}(0) - C_{eq}^{\alpha})\, e^{\frac{R_{C^{\alpha}} + R_{C^{\beta}}}{2}T}\left[e^{kT} - \left(1 + \frac{R_{C^{\alpha}} - R_{C^{\beta}}}{2k}\right)\sinh(kT)\right]\right] + (C_{eq}^{\beta} - (C_z^{\beta}(0))\, e^{-\frac{R_{C^{\alpha}} + R_{C^{\beta}}}{2}T}\, \frac{\sigma_{C^{\alpha}C^{\beta}}}{k}\sinh(kT) \quad (6)$$

TABLE 1
DIPOLE–DIPOLE INTERACTION CONSTANT C^2_{AB} FOR INTERACTIONS BETWEEN $^{13}C^{\alpha}$ AND ADJACENT NUCLEI

Interaction nuclei	r (Å)	c^2_{AB} (10^9 s^{-2})	$c^2_{AB} / \Sigma c^2_{AB}$
C^{α}-H^{α}	1.10	5.084	0.942
C^{α}-C^{β}	1.54	0.043	0.008
C^{α}-H^{β}	2.03	0.129	0.024
C^{α}-N	1.46	0.009	0.002
C^{α}-H^{N}	2.15	0.091	0.016
C^{α}-C'	1.53	0.044	0.008

The following values are assumed: $h = 6.626 \cdot 10^{-34}$ Js, $\mu_0 = 4\pi \cdot 10^{-7}$ TmA, $\gamma_H = 2.6752 \cdot 10^8\ s^{-1}T^{-1}$, $\gamma_C = 6.728 \cdot 10^7\ s^{-1}T^{-1}$, $\gamma_N = 2.709 \cdot 10^7\ s^{-1}T^{-1}$.

where

$$k = \sqrt{\left(\frac{R_{C\alpha} - R_{C\beta}}{2}\right)^2 + \sigma^2_{C^{\alpha}C^{\beta}}}$$

The experiment performed for measuring T_1 records the ^{13}C chemical shift prior to the relaxation period T, so that $C^{\alpha}_z(0) \sim C^{\alpha}_{eq} \cos(\Omega_{C\alpha} t_1)$ and $C^{\beta}_z(0) \sim C^{\beta}_{eq} \cos(\Omega_{C\beta} t_1)$. Therefore, after 2D Fourier transformation the first term of Eq. 6 gives cross peaks at $(\Omega_{C\alpha},\Omega_{H\alpha})$ while the second term corresponds to cross peaks at $(\Omega_{C\beta},\Omega_{H\alpha})$. To eliminate the dependence of the relaxation rate on the equilibrium values of the longitudinal magnetization, the magnetization of alternate scans is stored on the +Z-axis and the –Z-axis at the beginning of the relaxation period T (Sklenář et al., 1987):

$$C^{\alpha}_z(T) \sim \underbrace{C^{\alpha}_z(0)\, e^{-\frac{R_{C\alpha}+R_{C\beta}}{2}T}\left[e^{kT} - \left(1 + \frac{R_{C\alpha} - R_{C\beta}}{2k}\right)\sinh(kT)\right]}_{(\Omega_{C^{\alpha}},\Omega_{H^{\alpha}})} - \underbrace{C^{\beta}_z(0)\, e^{-\frac{R_{C\alpha}+R_{C\beta}}{2}T}\,\frac{\sigma_{C^{\alpha}C^{\beta}}}{k}\sinh(kT)}_{(\Omega_{C^{\beta}},\Omega_{H^{\alpha}})} \qquad (7)$$

Since the second term of Eq. 7 is proportional to $\sigma_{C^{\alpha}C^{\beta}}$, only very weak cross peaks at $(\Omega_{C\beta},\Omega_{H\alpha})$ will be observed (Fig. 1). In protein applications considered so far we have not seen them at all. Expanding the first term of Eq. 7 in a power series of T:

$$C^{\alpha}_z(T) \sim C^{\alpha}_z(0) e^{-R_{C^{\alpha}}T}\left[1 + \frac{\sigma^2_{C^{\alpha}C^{\beta}} T^2}{2} + O(T^3)\right] \qquad (8)$$

it is easy to show that the contribution of the cross relaxation $\sigma_{C^{\alpha}C^{\beta}}$ to the value of the cross-peak intensity at $(\Omega_{C\alpha},\Omega_{H\alpha})$ is less than 8% for $\tau_C \leq 20$ ns and $T \leq 1/R_{C\alpha}$ (Fig. 1). For ribonuclease T1, with an overall correlation time of about 6 ns (Fushman et al., 1994), an error of no more than 2–4% in the measured values of $R_{C\alpha}$ should be obtained by fitting the experimental data to a single exponential. The smaller T_1 value of $^{13}C^{\alpha}$ of a labeled protein in comparison to its value in an unlabeled protein is mainly due to the additional terms $\rho_{C^{\alpha}C^{\beta}}$ and $\rho_{C^{\alpha}C'}$. For RNase T1, their contribution leads to T_1 values which are about 15% too small. It should be emphasised that this additional magnetization loss cannot be 'refocussed' by any pulse sequence. For proteins with a longer rotational correlation time, the contribution of $\rho_{C^{\alpha}C^{\beta}}$ and $\rho_{C^{\alpha}C'}$ to $R_{C\alpha}$ increases steadily. As a consequence, the T_1 relaxation time cannot be interpreted with an AX spin system for larger proteins.

The heteronuclear $^1H^{\alpha}$-$^{13}C^{\alpha}$ NOE is also influenced by the additional homonuclear ^{13}C dipole–dipole interactions. To quantify these effects, the heteronuclear NOE of C^{α} of alanine in a uniformly labeled protein is compared to its value in an unlabeled sample. Alanine seems to be a good test compound, because the large NOE value of the $^{13}C^{\beta}$-methyl group should have a significant influence on the NOE of $^{13}C^{\alpha}$. Cross relaxation takes place between H^{α} and C^{α}, between H^{β} and C^{β} and between C^{α} and C^{β}. Equation 9 describes these interactions:

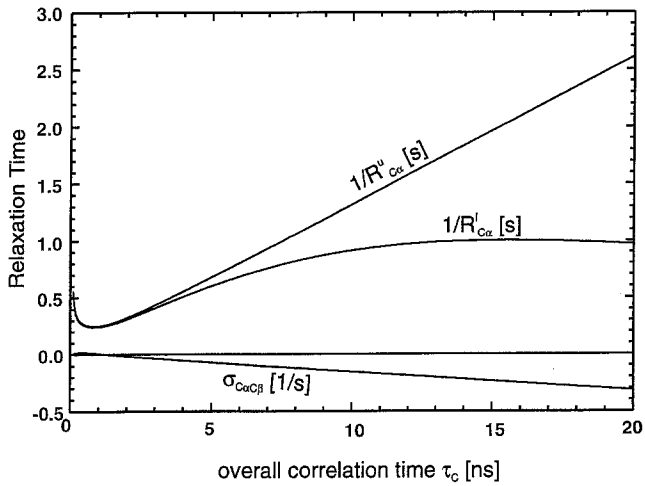

Fig. 1. Theoretical $^{13}C^{\alpha}$ relaxation times as a function of isotropic correlation time τ_C. Values for the direct dipole relaxation time ($1/R_{C\alpha}$) in an unlabeled protein sample ($1/R^u_{C\alpha}$) and in a uniformly enriched protein ($1/R^l_{C\alpha}$) are indicated. The cross-relaxation rate $\sigma_{C^{\alpha}C^{\beta}}$ is also shown. In the calculation, isotropic tumbling of a rigid molecule is assumed and its spectral density function is given by $J(\omega) = 2/5\ [\tau_C / (1 + (\omega\tau_C)^2)]$ at 600 MHz.

$$\begin{pmatrix} \frac{d}{dt}C_z^\alpha \\ \frac{d}{dt}C_z^\beta \end{pmatrix} = \begin{pmatrix} -\sigma_{H^\alpha C^\alpha} & -R_{C^\alpha} & -\sigma_{C^\alpha C^\beta} & 0 \\ 0 & -\sigma_{C^\alpha C^\beta} & -R_{C^\beta} & -n\sigma_{H^\beta C^\beta} \end{pmatrix} \times \begin{pmatrix} \langle H_z^\alpha \rangle - H_{eq}^\alpha \\ \langle C_z^\alpha \rangle - C_{eq}^\alpha \\ \langle C_z^\beta \rangle - C_{eq}^\beta \\ \langle H_z^\beta \rangle - H_{eq}^\beta \end{pmatrix} \quad (9)$$

where $R_{C\alpha} = \rho_{H\alpha C\alpha} + \rho_{C\alpha C\beta} + \rho_{C\alpha C'}$ and $R_{C\beta} = \rho_{C\alpha C\beta} + n\rho_{H\beta C\beta}$; n denotes the number of protons covalently bound to C^β. For steady-state conditions, the heteronuclear NOE of C^α can be derived from Eq. 9 assuming that H^α and H^β are saturated ($\langle H_z^\alpha \rangle = \langle H_z^\beta \rangle = 0$). For the NOE of $^{13}C^\alpha$, Eq. 10 is obtained:

$$\frac{C_z^\alpha}{C_{eq}^\alpha} = 1 + \frac{\gamma_C}{\gamma_H} \frac{1}{R_{C^\alpha}\left[1 - \frac{\sigma_{C^\alpha C^\beta}^2}{R_{C^\alpha} R_{C^\beta}}\right]} \times \left[\sigma_{H_\alpha C_\alpha} - \frac{n_\beta \cdot \sigma_{C^\alpha C^\beta} \cdot \sigma_{H^\beta C^\beta}}{R_{C^\beta}}\right] \quad (10)$$

For a quantification of the heteronuclear NOE, the spectral density function derived from the model-free approach of Lipari and Szabo (1982) is used in order to describe the dynamic behaviour of the C^α-H^α- and the C^α-C'-bonds. For the methyl group a modified spectral density function is applied, taking into account the rapid methyl jump rate around the C^α-C^β-bond (S_f^2,τ_f) and the reorientation of the C^α-C^β-bond (S_s^2,τ_s) on a time scale intermediate between the methyl jump rate and the overall tumbling rate (Clore et al., 1990a,b). The comparison of the heteronuclear NOE of C^α in labeled, selectively labeled and unlabeled alanine is shown in Fig. 2. For the unlabeled alanine Eq. 10 was used, assuming that $\sigma_{C^\alpha C^\beta} = 0$. Since the τ_C value of RNase T1 was assumed to be 6 ns, the difference of the C^α NOE value of labeled and unlabeled alanine is less than 5%. The experimental errors should not be more than 5–10% of the absolute value, and hence it seems justified to describe C^α-H^α as an AX spin system for the determination of C^α NOE values.

From the above outline it appears obvious that the transverse relaxation of aliphatic ^{13}C nuclei is dominated by their interaction with the covalently bound hydrogen(s) and hence, with respect to their relaxation behaviour these carbons can be described as AX (methine group), AX_2 (methylene group) and AX_3 (methyl group) spin systems. For the longitudinal relaxation rate and the heteronuclear NOE, contributions of both the heteronuclear ^{13}C-^1H interaction(s) and the homonuclear ^{13}C-^{13}C interaction(s) have to be considered. The ratio of their contributions mainly depends on the overall correlation time; in fact, for small proteins the heteronuclear interaction dominates and isolated AX, AX_2 and AX_3 spin systems can be assumed. With larger rotational correlation times the contribution of homonuclear interactions increases, and the relaxation of neighboring aliphatic ^{13}C nuclei has to be considered in a multispin system.

Simulation and optimization of the transverse relaxation period

The simulation of the T_2 relaxation delay is based on a system consisting of two J-coupled nuclei S_1 and S_2 with resonance offsets Ω_1 and Ω_2. The entire Hamiltonian during a free precession time interval in the rotating frame is

$$H_f = \Omega_{S1}S_{1z} + \Omega_{S2}S_{2z} + 2\pi J_{CC}\vec{S}_1 \cdot \vec{S}_2 \quad (11)$$

During an rf pulse of amplitude γB_1 and phase x the Hamiltonian takes the form

$$H_p = H_f + \gamma B_1 S_x \quad (12)$$

In case the Hamiltonian is time independent, the solution of the Liouville von Neumann equation, which describes the time evolution of the spin density matrix, takes the simple form:

$$\sigma(t + \tau) = e^{-iH\tau}\,\sigma(t)e^{iH\tau} = U \cdot \sigma(t) \cdot U^{-1} \quad (13)$$

It has to be noted that throughout the entire CPMG pulse sequence the time independence of the Hamiltonian is not fulfilled, but it is constant during some time periods.

In order to characterize the quality of the CPMG and

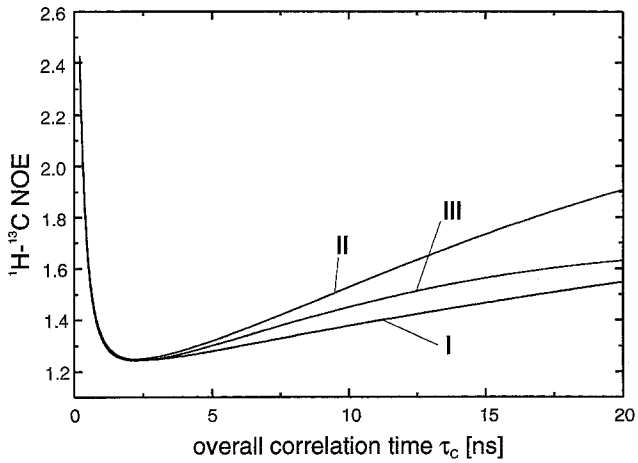

Fig. 2. ^1H-$^{13}C^\alpha$ heteronuclear NOE of an alanine residue as a function of τ_C. Curve I corresponds to an unlabeled sample, while curves II and III show the corresponding NOE-τ_C relation in a selectively enriched ($^{13}C^\alpha$, $^{13}C^\beta$) alanine residue and a uniformly enriched ($^{13}C^\alpha$, $^{13}C^\beta$, $^{13}C'$) alanine residue, respectively. The following parameters are assumed: (i) for the C^α-H^α-bond: $S_{CH}^2 = 0.9$, $\tau_{CH}^i = 50$ ps; (ii) for the C^α-C'-bond: $S_{C\alpha C'}^2 = 0.9$, $\tau_{C\alpha C'}^i = 1$ ns; (iii) for the methyl group: $S_f^2 = 0.111$, $S_s^2 = 0.9$, $\tau_f = 20$ ps, $\tau_s = 1$ ns.

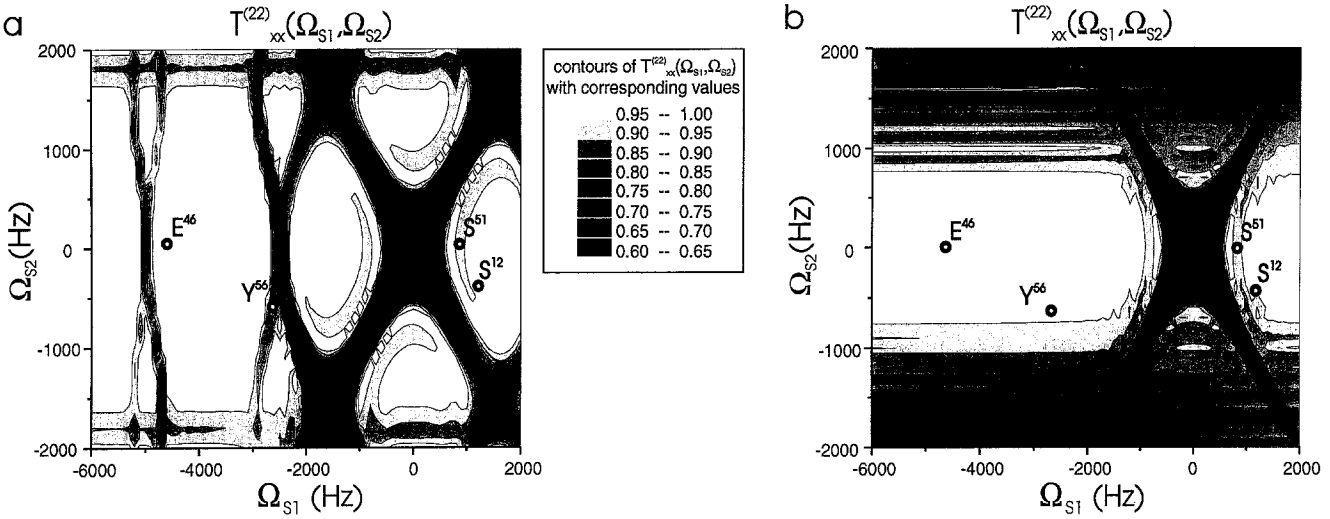

Fig. 3. Auto transfer efficiency $T^{(22)}_{xx}$ as a function of Ω_{S_1} and Ω_{S_2} for (a) 2δ = 350 μs (τ_{CPMG} = 12.6 ms) and (b) 2δ = 0 (τ_{CPMG} = 12.8 ms). In (a) an rf field amplitude of 5000 Hz was used for ^{13}C 180° pulses while in (b) a spin-lock field strength of 3125 Hz was chosen. A coupling constant of $J_{C\alpha C\beta}$ = 37 Hz was assumed (see text).

the spin-lock pulse sequences for the determination of T_2, two checking procedures were applied. The first procedure compares the position of the magnetization vector *after* the CPMG sequence with its position at the beginning by means of an 'auto transfer efficiency' $T^{(22)}_{xx}(\Omega_{S1}, \Omega_{S2}, \tau_{CPMG})$. It is a measure for the transfer of the operator S_{2x} to itself as a function of the resonance offsets Ω_{S1} and Ω_{S2} and a specific CPMG time τ_{CPMG}:

$$T^{(22)}_{xx}(\Omega_{S1},\Omega_{S2},\tau_{CPMG}) = \mathrm{Tr}\left[S^{+}_{2x}\, U_{eff}(\Omega_{S1},\Omega_{S2},\tau_{CPMG})\, S_{2x} U^{-1}_{eff}(\Omega_{S1},\Omega_{S2},\tau_{CPMG})\right] \quad (14)$$

The propagator U_{eff} can be expressed by a sequence of unitary transformations $U_i(\tau_i)$ with time-independent Hamiltonians:

$$U_{eff}(\Omega_{S1},\Omega_{S2},\tau_{CPMG}) = \left[e^{-iH_f\delta}\cdot e^{-iH_p\tau_p}\cdot e^{-iH_f\delta}\right]^n \quad (15)$$

where 2δ is the delay between two 180° ^{13}C pulses and τ_p is their duration. The second procedure is a measure for the effective transverse relaxation $\Gamma^{(22)}$ of the magnetization vector S_2 *during* the CPMG sequence, as expressed in Eq. 16:

$$\Gamma^{(22)} = \frac{1}{\tau_{CPMG}} \int_0^{\tau_{CPMG}} \sqrt{\mathrm{Tr}\left[S_2^{+}(\Omega_{S1},\Omega_{S2},t)\cdot S_{2x}\right]^2 + \mathrm{Tr}\left[S_2^{+}(\Omega_{S1},\Omega_{S2},t)\cdot S_{2y}\right]^2}\, dt \quad (16)$$

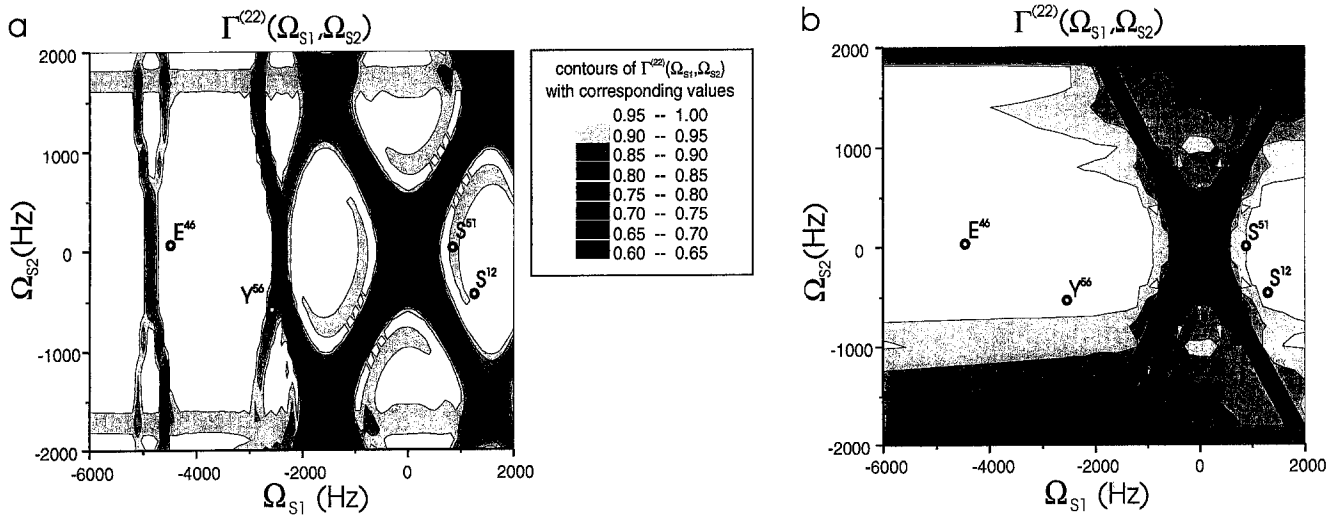

Fig. 4. Effective transverse relaxation $\Gamma^{(22)}$ as a function of Ω_{S_1} and Ω_{S_2} under the same conditions as in Fig. 3. The delay $\Delta t = \tau_{i+1} - \tau_i$ used in Eqs. 16 and 17 was set to 10 μs.

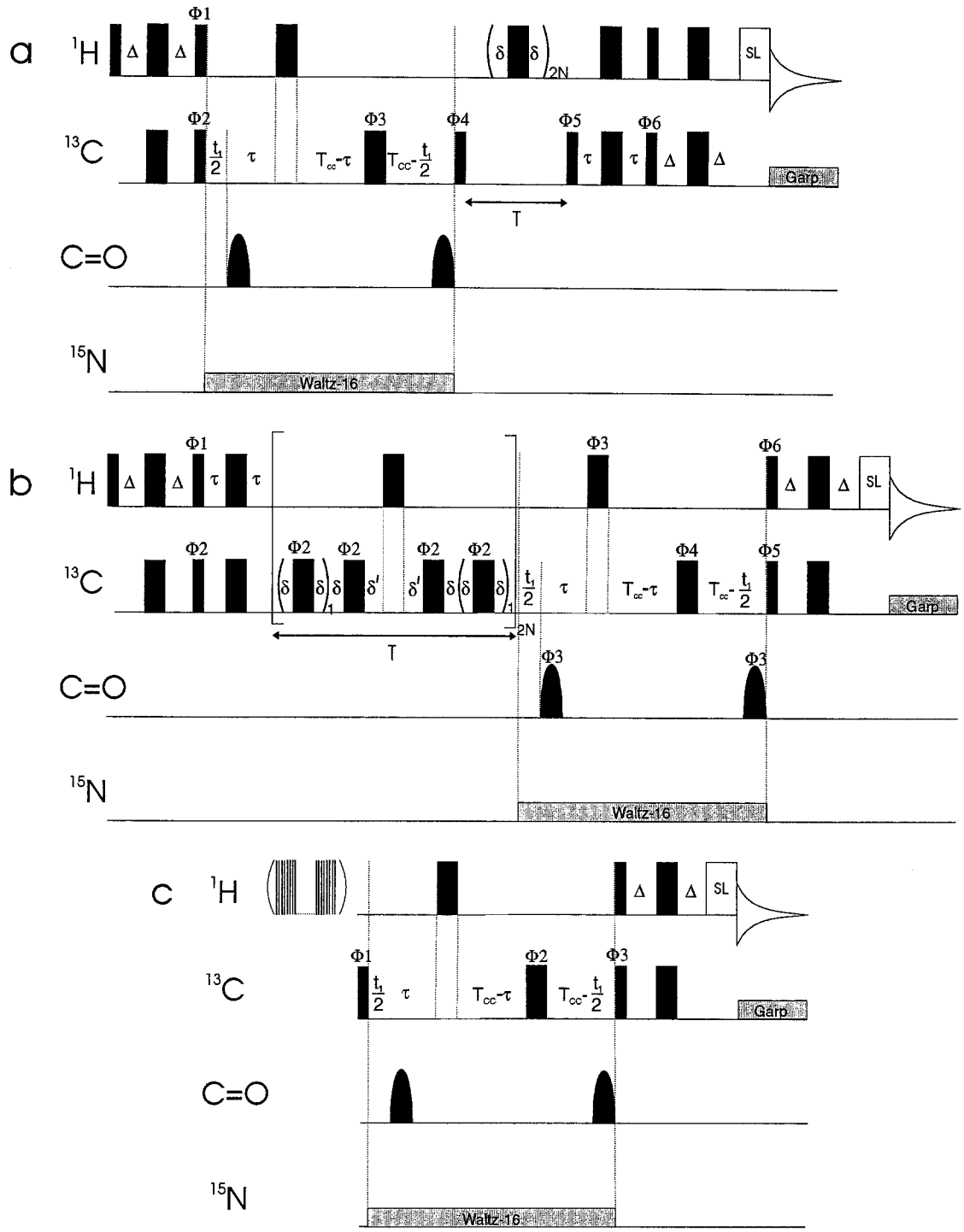

Fig. 5. Pulse sequences for the measurement of (a) $^{13}C^{\alpha}$ T_1, (b) T_2 and (c) heteronuclear NOE values with ^{1}H detection. All narrow pulses have a flip angle of 90°, the larger pulses have a 180° flip angle. Pulses for which the phase is not indicated are applied along the x-axis. The value for Δ and τ is set to $1/4J_{CH}$. A trim pulse of 1.5 ms is used just before aquisition to suppress the residual water signal and magnetization originating from protons not directly coupled to ^{13}C. The length of the constant-time period is set to $2T_{cc}$ = 27 ms. Except for measuring $T_{1\rho}$, the carrier was set to 59 ppm. Sinc-shaped phase-modulated off-resonance DANTE pulses with an rf field strength of 2500 Hz were used to excite the carbonyl carbons approximately 17.5 kHz downfield from the ^{13}C carrier. The ^{13}C pulses for the aliphatic absorption region were tuned to a value of $\gamma B_1 = \Delta\Omega_{C\alpha C'}/\sqrt{15}$, such that the carbonyl carbons are not affected. A composite 180° (90_x 180_y 90_x) pulse is used in the ct period to achieve complete inversion of all aliphatic carbon resonances. $^{13}C^{\alpha}$ decoupling during acquisition is achieved using GARP modulation with a field strength of 2.5 kHz and ^{15}N decoupling is accomplished by a WALTZ-16 scheme with an rf field of 900 Hz. The phase cycling used is as follows: (a) Φ1 = 8(y),8(–y); Φ2 = 4(x),4(–x); Φ3 = 8(x),8(–x),8(y),8(–y); Φ4 = y,–y; Φ5 = 2(x),2(–x); Φ6 = y; Acq. = (x,–x,–x,x),2(–x,x,x,–x),(x,–x,–x,x). (b) Φ1 = y,–y; Φ2 = 2(x),2(–x); Φ3 = 16(x),16(–x); Φ4 = 8(x),8(–x),8(y),8(–y); Φ5 = 8(x),8(–x); Φ6 = 4(x),4(–x); Acq. = (x,–x,–x,x),2(–x,x,x,–x),(x,–x,–x,x). For both (a) and (b) the receiver phase is inverted after 16 scans. Quadrature detection is achieved by TPPI of Φ4 for scheme (a) and Φ5 for scheme (b). (c) Φ1 = x,–x; Φ2 = 4(x),4(–x),4(y),4(–y); Φ3 = 2(y),2(–y); Acq. = 2(x,–x,–x,x),2(–x,x,x,–x); quadrature detection is achieved by TPPI of Φ1.

$\Gamma^{(22)}$ can be interpreted as the average of the projection of the magnetization vector S_2 onto the transverse plane. In practice, the integration is substituted by a summation and the trajectory $S_2(\Omega_{S_1}, \Omega_{S_2}, t)$ can be calculated assuming that the influence of relaxation can be neglected (Griesinger et al., 1988):

$$S_2(\Omega_{S1}, \Omega_{S2}, t_{i+1}) = U_i \cdot S_2(\Omega_{S1}, \Omega_{S2}, t_i) \cdot U_i^{-1} \qquad (17)$$

with $S_2(\Omega_{S1}, \Omega_{S2}, 0) = S_{2x}$, where U_i is the propagator for a part of the free precession time interval or for a part of the rf pulse. For the design of the pulse sequences the conditions $T_{xx}^{(22)} = 1$ and $\Gamma^{(22)} = 1$ over a bandwidth as large as possible should be maintained.

Figure 3 depicts $T_{xx}^{(22)}$ as a function of Ω_{S_1} and Ω_{S_2} for $2\delta = 350$ ms (a) and $2\delta = 0$ (b) and $\tau_{CPMG} = 1/2J_{C^\alpha C^\beta}$, while Fig. 4 shows $\Gamma^{(22)}$ as a function of Ω_{S1} and Ω_{S2} under the same conditions as in Fig. 3. It is evident from these figures that for both δ values the homonuclear Hartmann–Hahn transfer ($S_{2x} \rightarrow S_{1x}$) takes place on-resonance, such that C^α T_2 relaxation times of amino acids, the C^α and C^β chemical shifts of which are similar, cannot be determined in a reliable manner. In cases where S_2 is on-resonance and S_1 is off-resonance, $T_{xx}^{(22)}$ and $\Gamma^{(22)}$ are nearly 1 and the parameters depend only slightly on Ω_{S_1}, Ω_{S_2} and τ_{CPMG}. Hence the measured T_2 values should be fairly reliable. From a comparison of contour plots of $T_{xx}^{(22)}$ and $\Gamma^{(22)}$ with various δ delays and rf field strengths, it appears obvious that the position of the side bands depends on δ while their structure and contour levels are determined by the rf field strength. If δ decreases, the frequency distance between the carrier position and the side bands increases to such an extent that for $\delta = 0$ the first side band moves to infinity. A comparison between Figs. 3a/4a and Figs. 3b/4b illustrates this effect and hence the spin-lock sequence seems to be more suitable for measuring T_2 than the CPMG sequence.

Experimental

In order to verify the theoretical considerations described above experimentally, we measured $^{13}C^\alpha$ T_1, T_2 and NOE values of 2 mM ribonuclease T1, uniformly $^{13}C/^{15}N$-labeled, dissolved in 99.996% D_2O at pD 5.5. Spectra were recorded on a Bruker AMX-600 spectrometer at 308 K.

The pulse sequences developed for measuring the relaxation rates based on ^{15}N experiments (Kay et al., 1992) are depicted in Fig. 5. In order to refocus the couplings of C^α to H^α, ^{15}N, C' and C^β during the t_1 evolution period, a constant-time evolution period was used (Vuister and Bax, 1992). In addition, the refocussing part of the INEPT magnetization transfer was integrated in the ct period such that antiphase magnetization at the beginning is converted to in-phase magnetization with respect to ^1H at the end and vice versa.

In order to measure T_1, the inversion-recovery scheme was used. To minimize cross-correlation effects between ^1H-^{13}C dipolar and CSA interactions, ^1H 180° pulses were applied every 5 ms (Boyd et al., 1990). As described above, phase alternation of $\Phi 4$ leads to a magnetization decay $\exp(-t/T_1)$. In this way a less optimal delay between scans will only affect the sensitivity of the experiment, without introducing systematic errors (Sklenář et al., 1987).

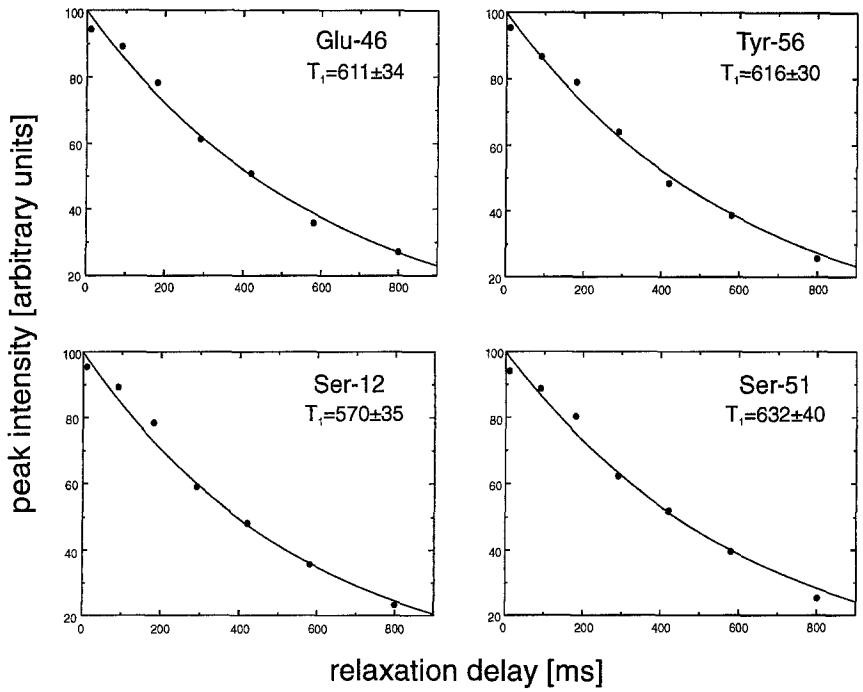

Fig. 6. Experimental and calculated intensity decay curves for the longitudinal relaxation of $^{13}C^\alpha$ of four resonances of ribonuclease T1.

For measuring T_2, a modified CPMG sequence with a ^1H 180° pulse at the top of the spin echo was used every 1.4 ms to suppress cross-correlation effects (Kay et al., 1992; Palmer et al., 1992). Within the CPMG sequence, a delay between ^{13}C 180° pulses of 350 ms was applied to ensure that ^{13}C magnetization remains in-phase with respect to ^1H, C' and ^{15}N and that no magnetization loss occurs due to C^{α}-C^{β} coupling for the duration of the CPMG interval. The carrier was set in the center of the $^{13}C^{\alpha}$ region, so that the maximal frequency offset was 1200 Hz.

In order to obtain $T_{1\rho}$, the delay δ in the CPMG sequence was set to zero and the rf field strength for the ^{13}C 180° pulses was tuned to $\gamma B_1 = \Delta\Omega_{C\alpha C'}/\sqrt{35}$. To achieve a tip angle between 80° and 90° for all C^{α} resonances, three series of 2D spectra with carrier positions at 54, 59 and 64 ppm were recorded.

In order to determine ^1H-^{13}C NOEs, data sets with and without ^1H saturation were collected. Scheme c in Fig. 5 indicates the sequence used for the data set with ^1H saturation. In this case a relaxation delay of 2.5 s was used,

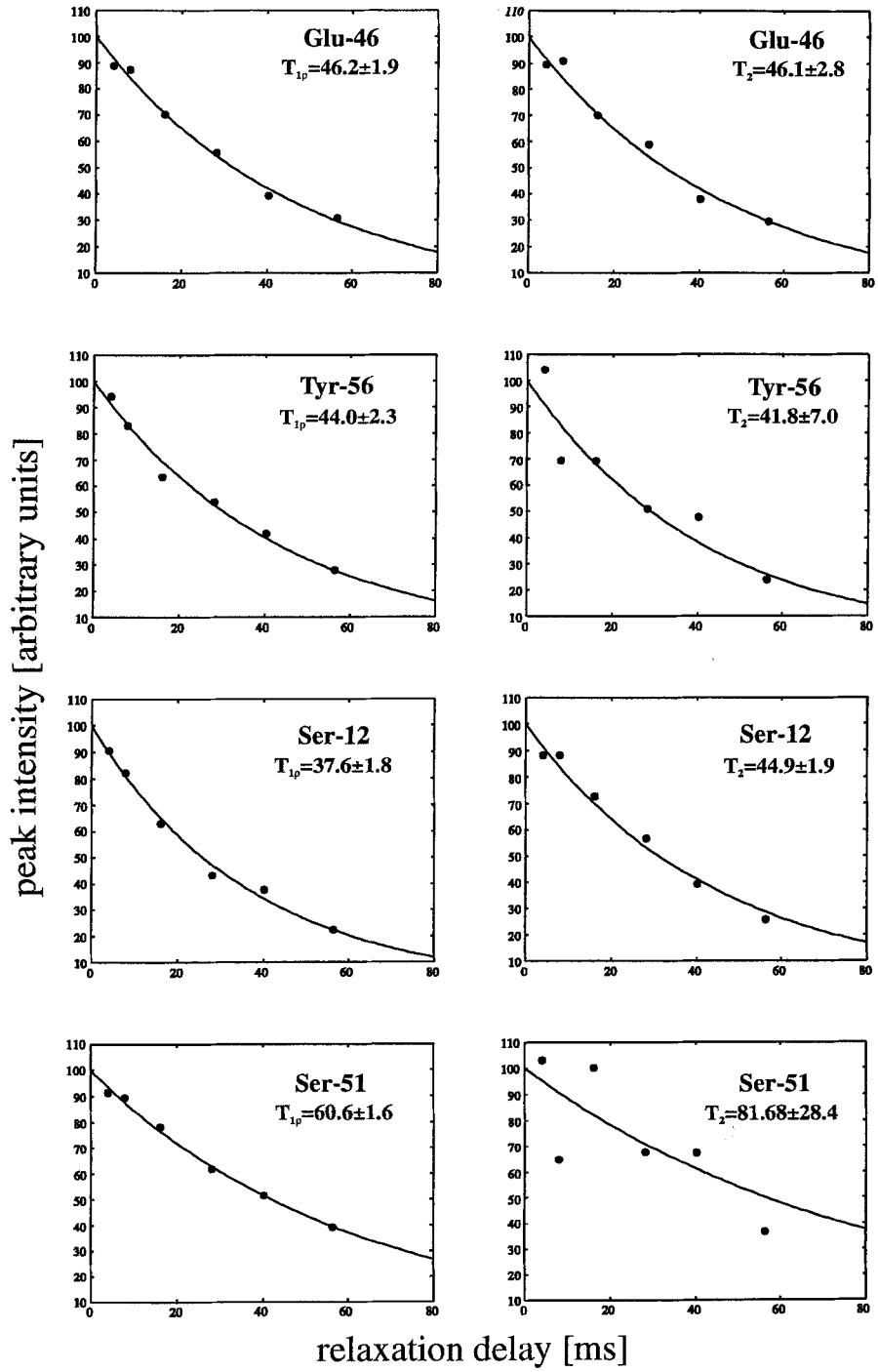

Fig. 7. Experimental and calculated intensity decay curves for determining T_2 of $^{13}C_{\alpha}$ of four amino acid residues of ribonuclease T1. The curves on the left side were obtained using a spin-lock sequence, while the curves on the right side were recorded with a CPMG sequence.

followed by proton presaturation during 3.5 s prior to the first ^{13}C pulse. For spectra with missing NOEs, a delay of 6 s was employed between scans.

All data sets were recorded as 320 × 2048 real matrices with 32 scans per t_1 point and spectral widths of 6000 Hz in F1 and 5120 Hz in F2. Apodization, zero-filling and Fourier transformation resulted in a digital resolution of 2.9 Hz/point in F1 and 2.5 Hz/point in the F2 dimension. For partially overlapped peaks, mirror-image linear prediction to 512 points in F1 was used prior to the other processing steps. The spectra were processed and analysed on a Bruker X32 workstation using the UXNMR and AURELIA programs (Bruker Analytische Messtechnik GmbH, Karlsruhe).

In order to obtain T_1 relaxation rates, seven spectra were acquired with T delays of 10, 90, 180, 290, 420, 580 and 800 ms. T_2 as well as $T_{1\rho}$ values were obtained from six spectra, acquired with T delays of 4, 8.1, 16.1, 28.2, 40.2 and 56.3 ms. For the evaluation of relaxation times the intensities of corresponding resonances in this series of 2D spectra were fitted to a single exponential, depending on the relaxation delay. The fit was performed using a least-squares minimisation procedure based on a downhill-simplex algorithm (Press et al., 1988) and the margin of errors was determined by a Monte Carlo approach, using the method of simulated experimental data (Kamath and Shriver, 1989). NOE values were obtained from the ratio of two peak volumes recorded with and without presaturation. The margin of errors was determined according to Nicholson et al. (1992).

Results and Discussion

Since C^α of glycine residues relax in a different manner (vide supra), these residues were not considered in this analysis. Of the remaining 94 amino acids, 89 C^α carbon residues could be assigned as single nonoverlapping peaks in the 2D ct-HSQC spectrum after linear prediction treatment. For four resonances of ribonuclease T1, typical decays as well as their best fits for the longitudinal relaxation are shown in Fig. 6. The values of the heteronuclear NOE for these resonances are 1.13 ± 0.09 for Glu^{46}, 1.18 ± 0.05 for Tyr^{56}, 1.20 ± 0.1 for Ser^{12} and 1.15 ± 0.06 for Ser^{51}. Reliable values with an error margin smaller than 10% were obtained for T_1 and for the heteronuclear NOE for 82 and 79 C^α carbons, respectively.

As described above, a CPMG sequence and a spin-lock were used in order to determine the transverse relaxation time. The quality of the data is demonstrated in Fig. 7 with typical decays for four resonances and with their best fits. For a comparison of the experimental data with the results of the numerical simulation, the C^α-C^β ^{13}C chemical shift combination for each of the four resonances is indicated in Figs. 3 and 4. For Glu^{46} and Ser^{12}, the simulation predicts that both pulse schemes should effectively suppress the magnetization loss due to the scalar C^α-C^β coupling, which is well confirmed in the experiment. By using a spin-lock, the decay curve for Tyr^{56} fits well to a single exponential, while for the CPMG sequence the error is more pronounced. This result agrees well with the simulation that predicts a side band at the position of the specific C^α-C^β chemical shift of Tyr^{56} for the CPMG sequence. The resonance frequencies for C^α and C^β of Ser^{51} are similar, so that a fit with a large error is expected. This is only partially confirmed in the experiment, as shown in Fig. 7. Apparently, the numerical simulation describes the behaviour of a two-spin system during a multiple pulse sequence like CPMG in principle rather well, but the precise position of the side bands may vary slightly in these simulations. Therefore, the use of the spin-lock sequence for measuring the transverse relaxation rate seems to be a better choice than the CPMG sequence, but it should be applied with care to serine and threonine residues because their C^α-C^β ^{13}C chemical shift values are almost identical. A reliable $^{13}C^\alpha$ transverse relaxation time was obtained for 76 amino acids of ribonuclease T1.

Acknowledgements

We thank Stefan Geschwindner and Harald Thüring for the isotope labeling of the protein sample. We also thank the Deutsche Forschungsgemeinschaft for a Grant (Ru145/8-7). J.E. is recipient of a stipend from the Graduiertenkolleg 'Proteinstrukturen, Dynamik und Funktion' of the University of Frankfurt.

References

Barbato, G., Ikura, M., Kay, L.E., Pastor, R.W. and Bax, A. (1992) *Biochemistry*, **31**, 5269–5278.

Boyd, J., Hommel, U. and Campbell, I.D. (1990) *Chem. Phys. Lett.*, **175**, 477–482.

Bull, T.E. (1992) *Prog. NMR Spectrosc.*, **24**, 377–410.

Clore, G.M., Driscoll, P.C., Wingfield, P.T. and Gronenborn, A.M. (1990a) *Biochemistry*, **29**, 7387–7401.

Clore, G.M., Szabo, A., Bax, A., Kay, L.E., Driscoll, P.C. and Gronenborn, A.M. (1990b) *J. Am. Chem. Soc.*, **112**, 4989–4991.

Dellwo, M.J. and Wand, A.J. (1989) *J. Am. Chem. Soc.*, **111**, 4571–4578.

Fushman, D., Weisemann, R., Thüring, H. and Rüterjans, H. (1994) *J. Biomol. NMR*, **4**, 61–78.

Griesinger, C. and Ernst, R.R. (1988) *Chem. Phys. Lett.*, **152**, 239–247.

Henry, G.D., Weiner, J.H. and Sykes, B.D. (1986) *Biochemistry*, **25**, 590–598.

Kamath, U. and Shriver, J.W. (1989) *J. Biol. Chem.*, **264**, 5586–5592.

Kay, L.E., Jue, T., Bangerter, B. and Demou, P.C. (1987) *J. Magn. Reson.*, **73**, 558–564.

Kay, L.E., Torchia, D.A. and Bax, A. (1989) *Biochemistry*, **28**, 8972–8979.

Kay, L.E., Nicholson, L.K., Delaglio, F., Bax, A. and Torchia, D.A. (1992) *J. Magn. Reson.*, **97**, 359–375.

Lipari, G. and Szabo, A. (1982) *J. Am. Chem. Soc.*, **104**, 4546–4559.

Neuhaus, D. and Williamson, M.P. (1989) *The Nuclear Overhauser Effect in Structural and Conformational Analysis*, VCH, New York, NY, pp. 39–40.

Nicholson, L.K., Kay, L.E., Baldisseri, D.M., Arango, J., Young, P.E., Bax, A. and Torchia, D.A. (1992) *Biochemistry*, **31**, 5253–5263.

Nirmala, N.R. and Wagner, G. (1988) *J. Am. Chem. Soc.*, **110**, 7557–7558.

Nirmala, N.R. and Wagner, G. (1989) *J. Magn. Reson.*, **82**, 659–661.

Palmer, A.G., Rance, M. and Wright, P.E. (1991) *J. Am. Chem. Soc.*, **113**, 4371–4380.

Palmer, A.G., Skelton, N.J., Chazin, W.J., Wright, P.E. and Rance, M. (1992) *Mol. Phys.*, **75**, 699–711.

Palmer, A.G., Hochstrasser, R.A., Millar, D.P., Rance, M. and Wright, P.E. (1993) *J. Am. Chem. Soc.*, **115**, 6333–6345.

Press, W.H., Flannery, B.P., Teukolsky, S.A. and Vetterling, W.T. (1992) *Numerical Recipes*, Cambridge University Press, Cambridge, pp. 402–404.

Richarz, R., Nagayama, K. and Wüthrich, K. (1980) *Biochemistry*, **19**, 5189–5196.

Sklenář, V., Torchia, D. and Bax, A. (1987) *J. Magn. Reson.*, **73**, 375–379.

Vuister, G.W. and Bax, A. (1992) *J. Magn. Reson.*, **98**, 428–435.

Ye, C., Fu, R., Hu, J., Hou, L. and Ding, S. (1993) *Magn. Reson. Chem.*, **31**, 699–704.